

Energetics of Halogen Bonding of Group 10 Metal Fluoride Complexes

Torsten Beweries,^{†,‡} Lee Brammer,[‡] Naseralla A. Jasim,[†] John E. McGrady,[§] Robin N. Perutz,^{*,†} and Adrian C. Whitwood[†]

[†]Department of Chemistry, University of York, Heslington, York, United Kingdom YO10 5DD

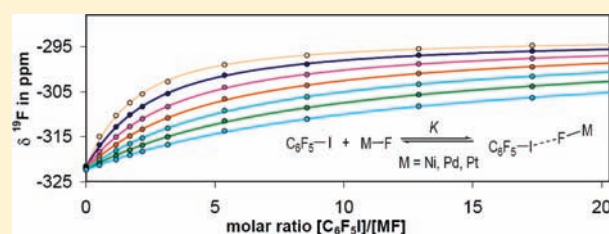
[‡]Department of Chemistry, University of Sheffield, Sheffield, United Kingdom S3 7HF

[§]Department of Chemistry, Inorganic Chemistry Laboratory, University of Oxford, South Parks Road, Oxford, United Kingdom OX1 3QR

S Supporting Information

ABSTRACT: A study is presented of the thermodynamics of the halogen-bonding interaction of C_6F_5I with a series of structurally similar group 10 metal fluoride complexes *trans*-[Ni(F)(2- C_5NF_4)(PCy₃)₂] (**2**), *trans*-[Pd(F)(4- C_5NF_4)(PCy₃)₂] (**3**), *trans*-[Pt(F)-{2- $C_5NF_2H(CF_3)$ }(PR₃)₂] (**4a**, R = Cy; **4b** R = *i*Pr) and *trans*-[Ni(F){2- $C_5NF_2H(CF_3)$ }(PCy₃)₂] (**5a**) in toluene solution. ¹⁹F NMR titration experiments are used to determine binding constants, enthalpies and entropies of these interactions ($2.4 \leq K_{300} \leq 5.2$; $-25 \leq \Delta H^\circ \leq -16$ kJ mol⁻¹; $-73 \leq \Delta S^\circ \leq -49$ J K⁻¹ mol⁻¹).

The data for $-\Delta H^\circ$ for the halogen bonding follow a trend Ni < Pd < Pt. The fluoropyridyl ligand is shown to have a negligible influence on the thermodynamic data, but the influence of the phosphine ligand is significant. We also show that the value of the spin–spin coupling constant J_{PF} increases substantially with adduct formation. X-ray crystallographic data for Ni complexes **5a** and **5c** are compared to previously published data for a platinum analogue. We show by experiment and computation that the difference between Pt–X and Ni–X (X = F, C, P) bond lengths is greatest for X = F, consistent with F(2p π)–Pt(5d π) repulsive interactions. DFT calculations on the metal fluoride complexes show the very negative electrostatic potential around the fluoride. Calculations of the enthalpy of adduct formation show energies of -18.8 and -22.8 kJ mol⁻¹ for Ni and Pt complexes of types **5** and **4**, respectively, in excellent agreement with experiment.



INTRODUCTION

Intermolecular interactions such as hydrogen and halogen bonding have found applications in various fields of chemistry and interdisciplinary sciences.^{1,2} The interactions of halogens are of great interest since they can exhibit both Lewis acidic and basic character. Structural characterization of these interactions is established in a wide range of situations encompassing organic compounds, main group elements, and transition metals.^{1a,3} In recent years, halogen bonding has emerged as a powerful, directional, and very useful noncovalent force relevant to molecular recognition with wide-ranging applications.² For example, the benefits of halogen bonding were described in a recent communication which showed that such an interaction can help to control the luminescence properties of bimetallic silver–gold clusters.⁴ Moreover, examples of the application of halogen bonding in self-assembly processes,⁵ in designing liquid crystals,⁶ in conducting materials,⁷ and in structural biology⁸ have been reported.

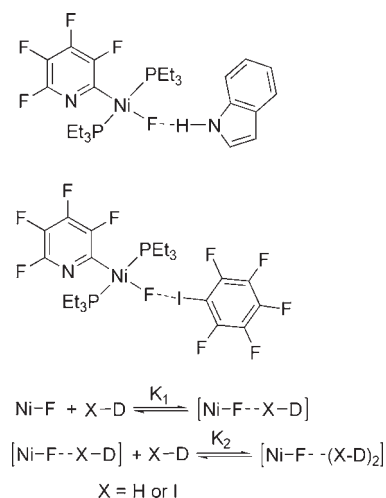
The phenomenon of halogen bonding has been studied for small gaseous molecules in detail by rotational spectroscopy⁹ and by computational methods, leading to a better understanding of this noncovalent force. Theoretical results suggest that halogen bonding results from interaction with the “ σ -hole”, an

electron-deficient region formed when polarizable halogen atoms are bound to electronegative groups as in C_6F_5I .¹⁰ Reports of the energetics of halogen bonding in solution are very limited indeed, although there was indirect evidence from crystal structures that halogen bonds compete successfully with hydrogen bonds.^{5,11} Laurence et al. assumed that relationships of shifts in IR bands observed on hydrogen bonding could be transferred to halogen bonds in order to determine trends in enthalpies of complexation.¹² Corradi et al. obtained the first calorimetric estimate of the enthalpy of adduct formation by adding 1-iodoperfluorohexane to excess tetramethylpiperidine, obtaining a value of 31 kJ mol⁻¹, assuming that solvent effects were negligible.^{5a} Very recently, the free energies of halogen bonding of a variety of substituted iodoperfluoroarenes to organic bases were reported, and subtle differences from hydrogen bonding were detected.^{13a–c} The free energies, enthalpies, and entropies of complexation of toluene-*d*₈ with 1- C_3F_7I ($\Delta H^\circ = -2.9$ kJ mol⁻¹) and 2- C_3F_7I ($\Delta H^\circ = -2.7$ kJ mol⁻¹) were reported by ¹⁹F NMR spectroscopy while this article was under review. DFT calculations indicated that these adducts involve C–I $\cdots\pi$ interaction.^{13d}

Received: April 11, 2011

Published: August 18, 2011

Chart 1. Hydrogen and Halogen Bonding of *trans*-[Ni(F)(C₅NF₄)(PEt₃)₂] (D = Hydrogen-Bond Donor or Halogen-Bond Donor)



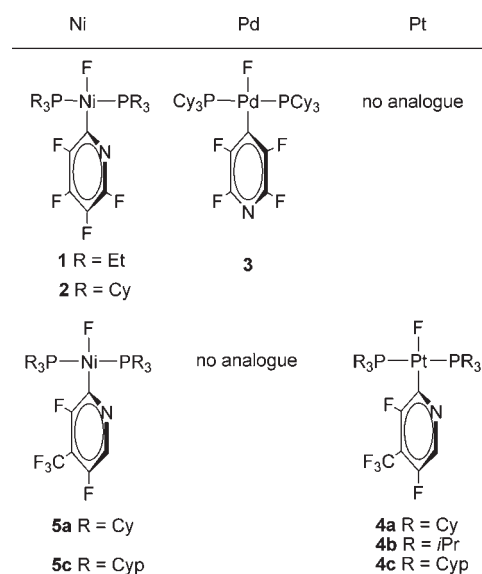
Our recent determination of the enthalpy, entropy, and temperature-dependent equilibrium constants of formation of halogen-bonded adducts between a nickel fluoride complex and iodopentafluorobenzene remains the most detailed source for the thermodynamics of halogen bonding in solution.¹⁴ Transition metal fluorides have been studied extensively to elucidate their unusual reactivity and their role in C–F activation¹⁵ and C–F bond-formation processes.¹⁶ We showed that *trans*-[Ni(F)(C₅NF₄)(PEt₃)₂] (**1**) acts as a Lewis base in the formation of hydrogen and halogen bonds with hydrogen bond donors (e.g., indole) and halogen bond donors (e.g., iodopentafluorobenzene, Chart 1).¹⁴ The formation of the adducts was monitored by multinuclear NMR spectroscopy, and the thermodynamics of the interactions were quantified by using the ¹⁹F NMR shift of the metal fluoride as a spectroscopic handle. We found that the enthalpy of halogen bond formation was –16(1) kJ mol^{–1} in toluene but –26(1) kJ mol^{–1} in heptane. Entropies of adduct formation in the two solvents were –42(4) and –63(4) JK^{–1} mol^{–1}, respectively. The ¹⁹F NMR chemical shift changed by more than 20 ppm at low temperature on adduct formation, although other NMR parameters were unaffected. We were also able to compare the energetics of halogen bond formation to those for hydrogen bonding to the same complex. The hydrogen bonding results may be compared to previous measurements, including some on other metal fluoride complexes.¹⁷

In this article, we present a comparative study of halogen bonding between iodopentafluorobenzene and members of a series of structurally similar group 10 metal fluoride complexes in toluene solution. We show that the *halogen-bond* enthalpy increases down the series, Ni, Pd, Pt. We also determined experimental and calculated metal–fluorine bond lengths for closely related nickel and platinum complexes in order to elucidate the effect of the change of metal on *metal–fluorine* bonding.

RESULTS AND DISCUSSION

Our strategy in this paper is to synthesize a series of closely related metal fluoride complexes so that we can identify periodic trends in the thermodynamics of halogen bond formation. The synthesis of isostructural metal fluoride complexes has previously

Chart 2. Group 10 Metal Fluorides for Halogen Bonding and Structural Studies

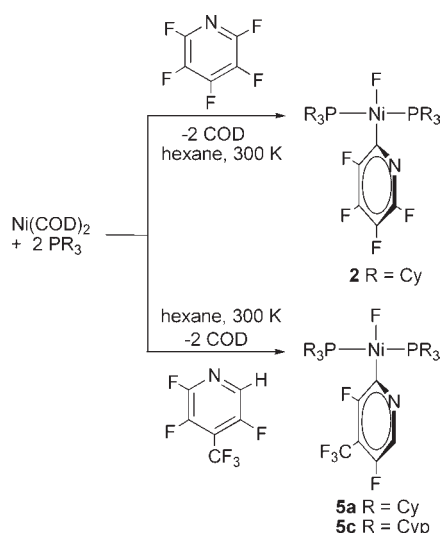


been reported only for binary complex ions, [MF₆]^{n–} and for complexes of early transition metals bearing *two* fluoride ligands.¹⁸ However, a series of such complexes bearing only *one* fluoride ligand is desirable for comparative studies of halogen bonding in order to avoid multiple interactions. Moreover, they should be soluble in nonpolar solvents in order to avoid competing interactions with the solvent. The synthesis of such a series has not been achieved previously.

We have shown that oxidative addition of aromatic C–F bonds at zero-valent group 10 metals can be used to generate a range of metal fluoride complexes. Oxidative addition of pentafluoropyridine proceeds smoothly with nickel(0) and palladium(0) in the presence of monodentate phosphines, and leads to C–F activation at the 2-position for nickel,¹⁹ but the 4-position for palladium (Chart 2).^{20a} Fluoride products can only be generated for platinum using 2,3,5-trifluoro-4-trifluoromethylpyridine; otherwise alkyl migration from the phosphine to the metal occurs with formation of a fluorophosphine ligand. Such reactions occur with Pt(PCy₃)₂ and pentafluoropyridine and involve a phosphine-assisted pathway with fluorine transfer from the pyridine to the phosphine.^{20b,21}

During our studies, we focused on group 10 metal fluorides and tried to synthesize a series of complexes by C–F activation with a minimum of structural differences. With these considerations in mind, we concentrated on square-planar complexes with two *trans*-tricyclohexylphosphine ligands (PCy₃) but with various fluoropyridyl groups *trans* to the fluoride ligand *trans*-[M(F)(py^F)(PCy₃)₂]. We synthesized two new nickel complexes by reaction with pentafluoropyridine and 2,3,5-trifluoro-4-trifluoromethylpyridine, yielding **2** and **5a**, respectively (Chart 2). The metal is bound at the 2-position of the fluoropyridyl in both these products. For the palladium derivative, we synthesized the previously described 4-tetrafluoropyridyl derivative, **3**, while for platinum we used the known compound **4a** derived from reaction with 2,3,5-trifluoro-4-trifluoromethylpyridine. This methodology provided us with a pair of structurally identical nickel and platinum complexes and a separate pair of very similar nickel and palladium complexes. Unfortunately, we were unable to

Scheme 1. Synthesis of Nickel Fluoride Complexes 2, 5a, and 5c



isolate the palladium analogues of **4a** and **5a**. The variations in the ligand set of complexes **2**, **3**, **4a**, and **5a** involve the fluoropyridyl group only. We have extended the series in two ways to allow us to explore the influence of the phosphine ligand in halogen bonding. Complex **2** could be compared to its triethylphosphine analogue **1** that was the subject of a previous communication,¹⁴ while complex **4a** can be compared to its triisopropylphosphine analogue **4b**.

The structural studies also required comparison of Pt complexes with the closest possible Ni analogues. We had previously determined the structure of the platinum bis(tricyclopentylphosphine) complex **4c**,^{20b} but crystals of **4a** (for which an exact Ni analogue exists) were of poor quality. To afford a direct comparison, we have therefore also synthesized the nickel analogue of **4c**, *trans*-[Ni(F){2-C₅NF₂H(CF₃)}(PCyP₃)₂] (**5c**) (Cyp = cyclopentyl).

Preparation of Nickel Fluoride Complexes and Structural Studies. The nickel fluorides **2**, **5a**, and **5c** were obtained directly from Ni(COD)₂ by reaction with two equivalents of the phosphine and the appropriate fluorinated pyridine in *n*-hexane, a protocol reported previously for other nickel monofluoride complexes (Scheme 1).¹⁹ Crystallization from *n*-hexane at −25 °C afforded yellow crystals of complex **2** suitable for X-ray analysis. Crystalline samples of compounds **5a** and **5c** were obtained from saturated toluene solutions at room temperature.

Complex **2** was assigned as a metal fluoride on the basis of the ¹⁹F resonance at δ −378.0. The four resonances due to the tetrafluoropyridyl fragment appear as multiplets of equal integration and resemble those of the known complex **1**.¹⁹ A doublet was observed in the ³¹P NMR spectrum at δ 19.3 (*J*_{PF} = 39 Hz) due to the two phosphines coupled to the fluoride ligand. The presence of the nickel fluoride was demonstrated by mass spectrometry (LIFDI⁺), showing the molecular ion at *m/z* 787.6.²² The spectroscopic data of complex **5a** resemble those of **2** (¹⁹F: NiF δ −375.1 and ³¹P: PCy₃ δ 19.0, *J*_{PF} = 37 Hz). The ¹H NMR signal of the trifluoromethyl-substituted pyridine ligand was observed downfield at δ 8.50, which is close to the value found before in the isostructural Pt complex (δ 8.54).^{20b} The electron-withdrawing nature of the CF₃ group causes a

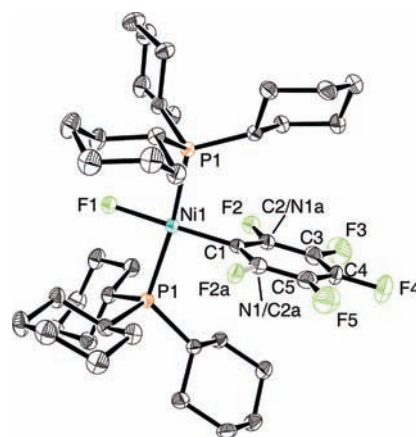


Figure 1. Molecular structure of complex **2**. Hydrogen atoms are omitted for clarity. The displacement ellipsoids correspond to 50% probability. Selected bond lengths (Å) and angles (deg.): Ni(1)–F(1) 1.8518(15), Ni(1)–P(1) 2.2300(4), Ni(1)–C(1) 1.865(2); F(1)–Ni(1)–P(1) 87.358(13), P(1)–Ni(1)–C(1) 92.892(14).

downfield shift of the signals of the fluorine atoms bound in *o*- and *p*-positions to the metal atom relative to the corresponding signals of **2**. As for compound **2**, the molecular ion was observed using LIFDI⁺ mass spectrometry (*m/z* 819.4). Complex **5c** was synthesized similarly, and its spectra are illustrated in the Supporting Information (Figures S9 and S10) (SI).

The molecular structures of complexes **2**, **5a**, and **5c** are shown in Figures 1 and 2. The nickel centers are coordinated in a slightly distorted square-planar geometry. There is disorder between N(1) and C(4)–F(5) in complex **2** which corresponds to rotation about Ni(1)–C(1), as found in analogues studied previously. The CF₃ group in each of **5a** and **5c** is also disordered. In addition, there is a ring-flip disorder in the cyclopentyl groups of **5c**. Bond distances and angles are in the expected range. Notably, Ni–F distances (Ni(1)–F(1) 1.8518(15), 1.8551(11), and 1.8591(10) Å for **2**, **5a**, and **5c**, respectively) are similar to those found for other square-planar nickel monofluoride complexes (e.g., 1.856(2) Å in *trans*-[Ni(F)(C₅NHF₃)(PET₃)₂]).¹⁹ The nickel–fluorine bonds are significantly shorter than the M–F bonds in the similar palladium and platinum complexes **3** and **4c** (**2**: 1.8518(15), **3**: 2.041(3) Å,^{20a} **4c**: 2.0402(19) Å^{20b}). The angle between the coordination plane C(1)P(1)P(2)F(1) and the C₅N plane of the fluoropyridyl ring is 90.00° for **2**, 88.30(8)° for **5a**, and 83.43(6)° for **5c**.

A comparison of the structural data of complexes **5a** and **5c** with those of the known platinum tricyclopentylphosphine complex *trans*-[Pt(F){2-C₅NF₂H(CF₃)}(PCyP₃)₂] (**4c**)^{20b} (analogue of **4a**) nicely reveals the influence of the metal on the M–X distances. The lengthening of the M–F distance from nickel to platinum is more pronounced than the lengthening of the other bonds in the first coordination sphere (Table 1).²³ The formation and structures of bis(phosphine) substituted group 10 metal fluorides were investigated earlier by theoretical methods,²⁴ where the exceptional increase in the M–F bond length on replacing nickel by platinum was first predicted.^{24f} Table 1 includes a comparison of calculated structures of *trans*-[M(F){2-C₅NF₂H(CF₃)}(PMe₃)₂] (M = Ni, Pt) with the same pyridyl ligand as in the experimental systems **4** and **5** but a simplified phosphine. The differences Δ*d*_{calc} between the Pt and Ni bond lengths are remarkably close to the experimental data. These calculations are consistent

with our earlier studies that indicated that these Pt–F bonds are weaker than Ni–F bonds, in contrast to the usual trends where Pt–X (X = H, C, P) bonds are usually stronger than the corresponding Ni–X bonds.^{24f}

Halogen Bonding of Metal Fluoride Complexes and C₆F₅I. Titration experiments were carried out in protio-toluene using the series of structurally related metal fluoride complexes shown in Chart 2 (other than 5c) and C₆F₅I. The latter has been found to be a very good halogen bond donor due to the fluorination of

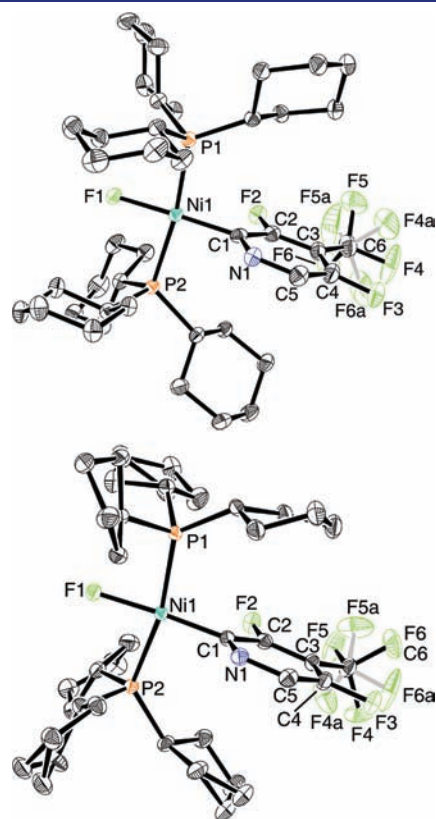
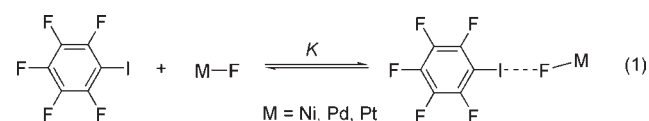


Figure 2. Molecular structures of complexes 5a (above) and 5c (below). Hydrogen atoms are omitted for clarity. The displacement ellipsoids correspond to 50% probability. Disorder of the CF₃ groups is shown for 5a and 5c. Three of the six cyclopentyl groups in 5c are also disordered. Selected bond lengths (Å) and angles (deg.): 5a Ni(1)–F(1) 1.8551(11), Ni(1)–P(1) 2.2249(5), Ni(1)–P(2) 2.2242(5), Ni(1)–C(1) 1.8732(19), C(1)–Ni(1)–P(1) 94.36(6), F(1)–Ni(1)–P(1) 87.66(4), C(1)–Ni(1)–P(2) 92.52(6), F(1)–Ni(1)–P(2) 85.62(4). 5c Ni(1)–F(1) 1.8591(10), Ni(1)–P(1) 2.2262(5), Ni(1)–P(2) 2.2299(5), Ni(1)–C(1) 1.8613(17), C(1)–Ni(1)–P(1) 96.09(5), F(1)–Ni(1)–P(1) 85.56(3), C(1)–Ni(1)–P(2) 95.32(5), F(1)–Ni(1)–P(2) 82.94(3).

Table 1. Comparison of M–X Bond Distances (Å) in Nickel and Platinum Fluoride Complexes *trans*-[M(F){2-C₅NF₂H(CF₃)}-(PR₃)₂] (M = Ni, R = Cy or Cyp; M = Pt, R = Cyp) by X-ray Crystallography and DFT-Optimized Structures for M = Ni, R = Me; M = Pt, R = Me

M–X	experimental distances/Å					calculated distances/Å		
	4c ^{20b}	5a	5c	$\Delta d_{\text{exp}}(4c-5a)$	$\Delta d_{\text{exp}}(4c-5c)$	M = Ni	M = Pt	Δd_{calc}
M–C	1.988(3)	1.8732(19)	1.8613(17)	0.115(4)	0.127(4)	1.91	2.00	0.09
M–F	2.0402(19)	1.8551(11)	1.8591(10)	0.185(2)	0.181(2)	1.83	2.05	0.22
M–P(1)	2.3224(8)	2.2249(5)	2.2262(5)	0.0975(9)	0.0992(9)	2.30	2.38	0.08
M–P(2)	2.3225(7)	2.2242(5)	2.2299(5)	0.0983(9)	0.0926(9)	2.31	2.37	0.06

the ring and the resulting high electrophilicity of the iodine atom.²⁵ Upon addition of the halogen bond donor, the ¹⁹F NMR fluoride signal of the corresponding metal fluoride of all the complexes exhibited a substantial downfield shift reaching ca. 10 ppm at room temperature and ca. 20 ppm at low temperature with excess C₆F₅I (Figure S11, SI). In contrast, the ¹⁹F resonances for the fluorinated pyridine ligand and the ³¹P NMR signals for the phosphine ligands remain almost unchanged (maximum change at room temperature 0.24 and 0.39 ppm, respectively). The ¹⁹F resonances of C₆F₅I are also shifted negligibly since C₆F₅I is present in excess. Thus, the formation of the halogen-bonded adduct can be monitored by ¹⁹F NMR spectroscopy using the fluoride resonance. The ratio of the metal fluoride to C₆F₅I concentrations was varied, giving titration curves that can be fitted using the simple model of eq 1 to yield the equilibrium constant for formation of the adduct *K* and the change in the ¹⁹F chemical shift between the free metal fluoride and the pure adduct ($\Delta\delta^{\text{fit}}$):



Thermodynamic data (ΔH° and ΔS°) can be obtained by recording titration curves at various temperatures and plotting $\ln K$ vs T^{-1} (Van't Hoff Plot). In all cases, the data could be fitted satisfactorily assuming exclusive formation of a 1:1 adduct. The 1:1 stoichiometry was confirmed by Job plots for complexes 2 and 4a. For the Job plots, we measured the change in chemical shift of the ¹⁹F resonance ($\Delta\delta$) as a function of the mol fraction of the metal complex (*X*) while keeping the sum of the concentrations [metal complex] + [C₆F₅I] = 0.01 mol dm⁻³. The graph of $X\Delta\delta$ vs *X* showed a maximum at *X* = 0.5 as anticipated for a 1:1 complex (Figures S1 and S6 in SI).²⁶ In our previous communication, the formation of a 1:2 adduct was observed when changing the solvent from toluene to *n*-heptane¹⁴ to prevent interaction of the perfluorinated arene with the π -electron system of the solvent molecules.²⁷ However, this was not possible for the examples described here due to the limited solubility of the metal fluorides in nonpolar solvents.

As an example, Figure 3 shows the titration data of the experiment using the system 2/C₆F₅I. The thermodynamic values for all experiments can be found in Table 2. All titration curves show a significant temperature dependence of the chemical shift caused by the interaction with the halogen bond donor. This effect is distinct for higher concentrations of C₆F₅I, whereas for lower concentrations the difference in chemical shifts is small. Analysis of the titration data gave excellent fits in all cases, resulting in Van't Hoff plots with correlation coefficients (*R*²) of

greater than 0.99 (Figure 4, see Figures S2–S5 and S7–S10 in SI for titration curves and Van't Hoff plots for other complexes).

In the titration experiment with complex **4a** and C_6F_5I , the platinum fluoride signal was absent for higher concentrations of C_6F_5I ($[C_6F_5I]/[4a] = 5.3$). Evidently, the platinum fluoride reacted with C_6F_5I to form a new complex, which has not been characterized yet. However, since the chemical shifts for low ratios of donor/metal fluoride determine the quality of the fit, thermodynamic parameters should still be reliable.

Complexes **4a** and **5a** differ only in the metal, but the results show a markedly higher binding enthalpy for platinum than for nickel. The palladium complex **3** has an enthalpy of formation that lies between the values of the nickel and platinum complex, but a direct comparison is not possible because its fluoropyridyl group differs from those in **4a** and **5a**. However, the nickel complexes **2** and **5a** offer an opportunity to determine independently the influence of the substitution pattern at the fluoropyridyl ligand on the thermodynamic parameters, since they have identical phosphines but different fluoropyridyl ligands. The difference in values for ΔH° and ΔS° for compounds **2** and **5a** is insignificant, suggesting that the influence of the different fluoropyridyl ligand on halogen bonding is negligible. Thus, a comparison of the tetrafluoropyridyl-substituted complexes **2** and **3** with complexes **4a** and **5a**, bearing a trifluoromethyl-substituted pyridine ligand is valid. These arguments enable us to deduce that the enthalpy of halogen bonding, $-\Delta H^\circ$, increases in the order Ni < Pd < Pt. There is evidence that $-\Delta H^\circ$ correlates with $-\Delta S^\circ$, leading to compensation in the values of ΔG° and K . However, the correlation is not close, and K_{300} varies as Ni \approx Pt < Pd,

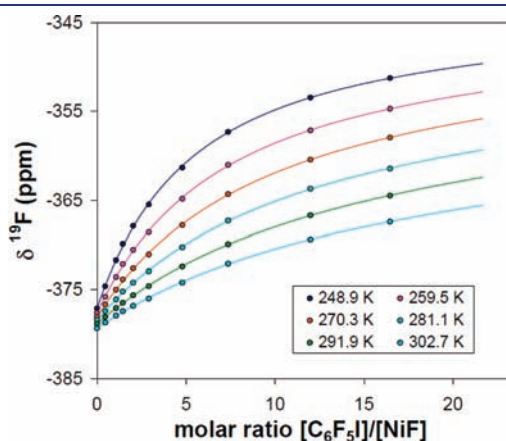


Figure 3. Fit of the titration curves at different temperatures, showing observed values for the ^{19}F chemical shift of the metal fluoride δ_F vs ratio of molar concentrations of C_6F_5I and complex **2**.

in contrast to the trend in $-\Delta H^\circ$. There is little change between the metals in the chemical shift difference between free metal fluoride and that of the adduct, $\Delta\delta^{fit}$ (Table 2).

The electronic influence of the phosphine substituents of the metal fluoride on halogen bonding was investigated by comparing nickel complexes **1** and **2** with PEt_3 and PCy_3 ligands, respectively, and by comparing platinum complexes **4a** and **4b** with PCy_3 and $PiPr_3$ ligands, respectively. In each pair the fluoropyridyl group is identical. The results show that the phosphine has a significant influence on ΔH° with the strongest binding for PCy_3 with both nickel and platinum (Table 2). The experimental titration data and the calculated thermodynamic data show that the difference in the chemical shifts $\Delta\delta$ is not correlated with the enthalpy and entropy.

The platinum complexes **4a** and **4b** offer the opportunity of monitoring the effect of halogen bonding on the value of the platinum–fluorine coupling constant for the metal fluoride resonance, J_{PtF} . The data for **4b** show that the measured J_{PtF} grows with increasing $[C_6F_5I]/[MF]$ and decreasing temperature (Figure 5). Although there is some scatter in the data due to broadening of the platinum satellites especially at low temperature and low $[C_6F_5I]/[MF]$, the upward trend is unmistakable. Because of the scatter in the data, we could not determine the equilibrium constant K and the limiting values of the coupling constant for the 1:1 adducts, J_{PtF}^{add} , independently. The data for 257, 268, and 279 K were fitted satisfactorily using the values of K at those temperatures derived from the chemical shift data, allowing us to determine J_{PtF}^{add} . This approach yielded values of J_{PtF}^{add} of 338 ± 27 , 363 ± 54 , and 392 ± 59 Hz, respectively, compared with 240–250 Hz for the free molecule in toluene solution, J_{PtF}^0 . Considering the large uncertainties in the values of J_{PtF}^{add} , it is not appropriate to draw any conclusions concerning the temperature dependence of J_{PtF}^{add} , but we can conclude

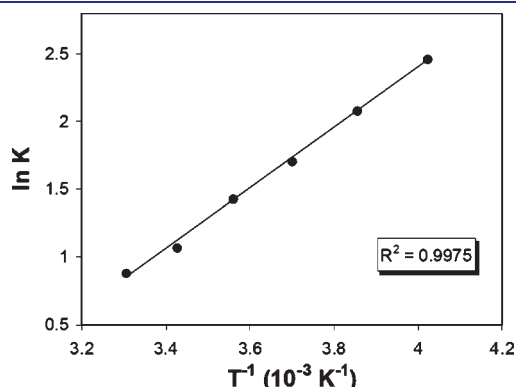


Figure 4. Van't Hoff plot for halogen bonding of C_6F_5I and complex **2**.

Table 2. Thermodynamic Data for Halogen Bonding of Group 10 Metal Fluorides with C_6F_5I in Toluene^a

Metal fluoride (MF)	ΔH° kJ mol ⁻¹	ΔS° J K ⁻¹ mol ⁻¹	K_{300}	K_{200} ^b	$\Delta\delta^{fit}_{303K}$ ^c
$[Ni(F)(2-C_3NF_4)(PEt_3)_2]$ (1) ¹⁴	-16(1)	-42(2)	3.41(9) ^a	96.6	33.7
$[Ni(F)(2-C_3NF_4)(PCy_3)_2]$ (2)	-18.6(4)	-54(2)	2.49(16)	109	36.0
$[Pd(F)(4-C_3NF_4)(PCy_3)_2]$ (3)	-21.7(4)	-59(1)	5.2(3)	385	35.5
$[Pt(F)\{2-C_3NF_2H(CF_3)\}(PCy_3)_2]$ (4a)	-24.5(11)	-73(4)	2.9(4)	385	37.9
$[Ni(F)\{2-C_3NF_2H(CF_3)\}(PCy_3)_2]$ (5a)	-18.9(4)	-54(1)	3.06(15)	130	35.6
$[Pt(F)\{2-C_3NF_2H(CF_3)\}(PiPr_3)_2]$ (4b)	-16.9(6)	-49(2)	2.4(2)	71.5	27.7

^a Errors are 95% confidence limits and are based on statistics of fits. ^b Extrapolated to 200 K. ^c $\Delta\delta^{fit}$ = Chemical shift difference between free metal fluoride and metal fluoride- C_6F_5I adduct, calculated by the fitting routine.

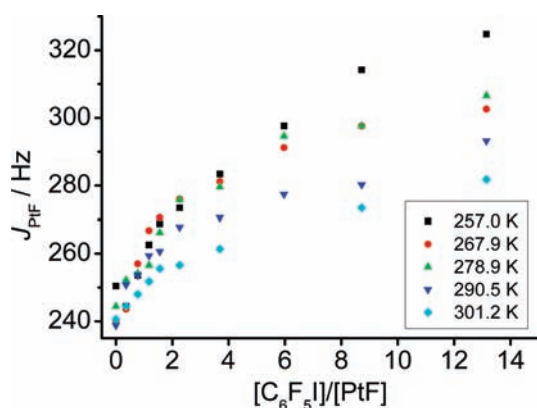


Figure 5. Plot of the spin–spin coupling constant J_{PtF} vs the concentration ratio $[\text{C}_6\text{F}_5\text{I}]/[\text{PtF}]$ for **4b** measured in toluene.

that formation of the $\text{C}_6\text{F}_5\text{I}\cdots\text{F}\text{-Pt}$ adduct results in a very large increase in J_{PtF} ($J_{\text{PtF}}^{\text{add}} \gg J_{\text{PtF}}^0$). The data for **4a** show similar trends, but the broadening is too severe for quantitative analysis.

Calculations on isotropic spin–spin coupling constants of binary metal fluorides have shown that both the Fermi Contact term and the paramagnetic spin–orbit term make major contributions to J_{MF} and that they may have opposite signs.²⁸ Thus, a simple inverse correlation between adduct strength and J_{PtF} is not to be expected.²⁹

Computational Studies of Halogen Bonding. The optimized structures (BHandHLYP) of the model metal fluoride complexes $\text{trans}[\text{Pt}(\text{F})\{2\text{-C}_5\text{NF}_2\text{H}(\text{CF}_3)\}(\text{PMe}_3)_2]$ and $\text{trans}[\text{Ni}(\text{F})\{2\text{-C}_5\text{NF}_2\text{H}(\text{CF}_3)\}(\text{PMe}_3)_2]$, along with their $\text{C}_6\text{F}_5\text{I}$ adducts, are summarized in Figure 6. The adduct geometries describe a $\text{C}\cdots\text{I}\cdots\text{F}\text{-M}$ halogen bond in which the halogen bond distance $\text{I}\cdots\text{F}$ is substantially shorter than the corresponding sum of van der Waals radii (3.45 Å)³⁰ ($\text{I}\cdots\text{F}(\text{Pt})$ 2.73 Å, R_{IF} 0.79; $\text{I}\cdots\text{F}(\text{Ni})$ 2.78 Å, R_{IF} 0.81).³¹ In both adducts the $\text{C}\cdots\text{I}\cdots\text{F}$ angles are close to linear (Pt 179°, Ni 180°). The $\text{I}\cdots\text{F}\text{-M}$ moiety is slightly bent for Ni (167°), but distinctly bent for Pt (145°). Such angles are consistent with observations in a survey of $\text{H}\cdots\text{F}\text{-M}$ angles for hydrogen bonding involving metal fluorides.^{1a} We note, also, that the $\text{I}\cdots\text{F}\text{-M}$ bending modes have very low frequencies. The formation of the adducts results in a lengthening of both $\text{M}\text{-F}$ and $\text{C}\text{-I}$ bonds, although the effects are marginal. Otherwise, the structures of both subunits remain unperturbed by the intermolecular interaction. The counterpoise-corrected interaction enthalpies (defined as $\Delta H(\text{adduct}) - \Delta H(\text{C}_6\text{F}_5\text{I}) - \Delta H(\text{complex})$) are -18.8 and -22.8 kJ mol^{-1} for Ni and Pt, respectively, in excellent agreement with the experimentally determined enthalpies of -18.9 and -24.5 kJ mol^{-1} for **5a** and **4a**, respectively. Thus, the observed trend toward stronger bonding in the platinum complex is reproduced by the calculations with the binding energy calculated to be 4.0 kJ mol^{-1} greater than that in the nickel analogue. Although this energy difference is small, the very similar structures of the two adducts under consideration means that sources of error (finite basis set, solvation) should be the same in both cases, providing some confidence that this number is meaningful.

Halogen bonding has usually been discussed in the context of an electrostatic model, whether referring to halogen bonds with $\text{M}\text{-X}$, $\text{X} = \text{Cl}, \text{Br}, \text{I}$,^{3h,i} or halogen bonds involving organic bases.^{12,13} We investigated an electrostatic model by calculating

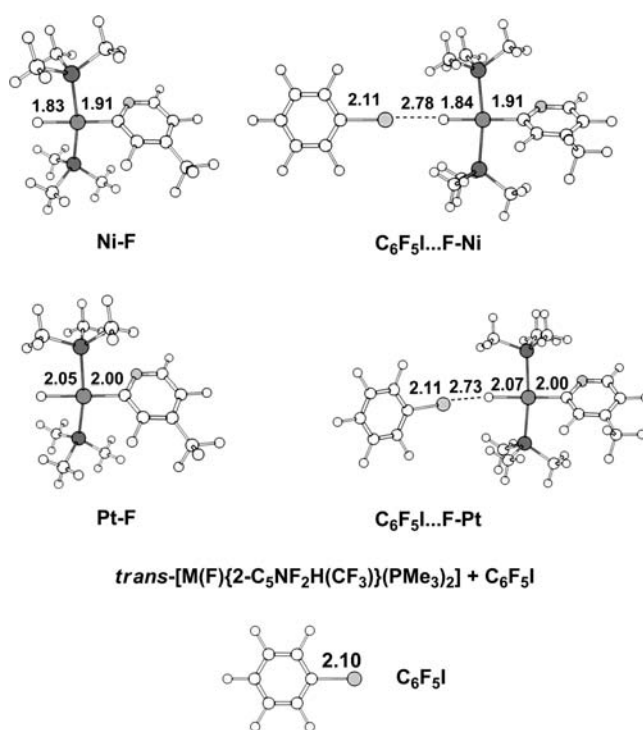


Figure 6. Optimized structures of $\text{trans}[\text{Ni}(\text{F})\{2\text{-C}_5\text{NF}_2\text{H}(\text{CF}_3)\}(\text{PMe}_3)_2]$, $\text{trans}[\text{Pt}(\text{F})\{2\text{-C}_5\text{NF}_2\text{H}(\text{CF}_3)\}(\text{PMe}_3)_2]$, and their $\text{C}_6\text{F}_5\text{I}$ adducts. Distances shown in Å.

the electrostatic potentials for the nickel and platinum complexes. On descending group 10 from Ni to Pt, we naturally anticipate an increase in metal–ligand bond lengths, but we have shown (both experimentally and computationally, see above) that $\text{M}\text{-F}$ bonds are affected to a greater extent than comparable $\text{M}\text{-C}$ bonds. This lengthening indicates that the $\text{Pt}\text{-F}$ bond is somewhat weaker than its $\text{Ni}\text{-F}$ counterpart, an effect that we ascribe to large $5d\pi\text{-}p\pi$ repulsions.^{24f,32} The electrostatic potentials (Figure 7) suggest that the region of negative potential around the fluoride ligand is slightly more radially extended in the platinum case, and the potential minimum along the extension of the $\text{M}\text{-F}$ vector is deeper for platinum fluoride (-302 kJ mol^{-1}) than nickel fluoride (-280 kJ mol^{-1}). Collectively, the differences allow for a more effective electrostatic interaction with the σ -hole of the iodine center in the case of the platinum fluoride.

A complementary perspective on halogen bonding can be obtained from an analysis of the topology of the electron density along the $\text{I}\cdots\text{F}$ axis.³³ In both nickel and platinum cases a bond critical point (BCP) is present between F and I, with a rather low electron density (~ 0.02 $\text{e}\text{Å}^{-3}$) and a positive value of the Laplacian, $\nabla^2\rho$, both of which are typical of closed-shell interactions. Significantly, however, the electron density at the critical point is marginally greater in the platinum case than in nickel (0.024 vs 0.020 $\text{e}\text{Å}^{-3}$). Sosa et al.³⁴ and Zou et al.³⁵ have independently established approximately linear relationships between electron density at the critical point and interaction energy in a series of halogen-bonded adducts, with gradients in the range 1400–1800 $\text{kJ}\text{Å}^3\text{mol}^{-1}\text{e}^{-1}$. Assuming a gradient of similar magnitude in this case, the difference in ρ of 0.004 $\text{e}\text{Å}^{-3}$ between nickel and platinum complexes equates to a difference in interaction energy of 5–7 kJ mol^{-1} , in excellent agreement with experiment and computed interaction energies. Thus, the subtle

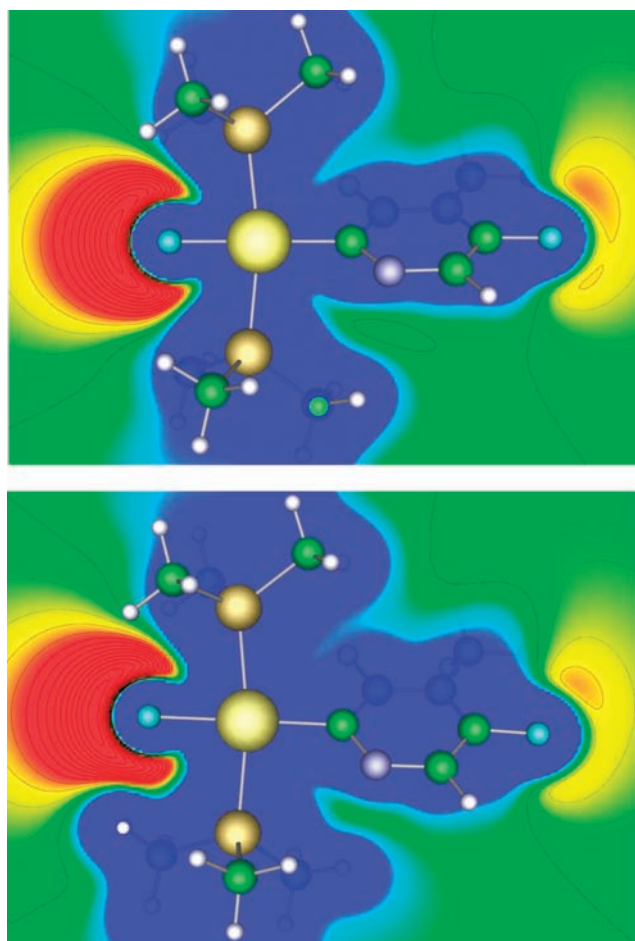


Figure 7. Electrostatic potentials in the metal coordination plane, shown with zero and negative contours at intervals of 5 kcal mol^{-1} (20.9 kJ mol^{-1}) for (upper panel) $\text{trans}[\text{Ni}(\text{F})\{\text{C}_5\text{NF}_2\text{H}(\text{CF}_3)\}_2(\text{PMe}_3)_2]$ and (lower panel) $\text{trans}[\text{Pt}(\text{F})\{\text{C}_5\text{NF}_2\text{H}(\text{CF}_3)\}_2(\text{PMe}_3)_2]$. Red indicates most negative potential, blue is most positive. Views in the plane of the pyridine ring are shown in Figure S14 (SI).

differences in interaction energy are consistent with the accumulation of greater charge in the intermolecular region in the platinum case.

CONCLUSION

We have established a series of structurally similar group 10 metal fluorides bearing two mutually trans PCy_3 ligands by synthesis of three new nickel fluoride complexes by C–F oxidative addition. The Ni and Pt complexes are isostructural, but the palladium complex has a different pyridyl substituent that results from a change in selectivity of the pathway of oxidative addition of the fluorinated pyridine.²⁰ We have examined quantitatively the extension of bond lengths for platinum compounds relative to related nickel compounds by experiment and computation. The biggest extension of the Pt–X bonds (X = C, P, F) relative to the Ni–X bonds is found for X = F, probably as a result of $p\pi-d\pi$ repulsive interactions.^{24f}

We have measured the ^{19}F NMR chemical shifts of these complexes dissolved in toluene in the presence of excess $\text{C}_6\text{F}_5\text{I}$ from 250 to 300 K and used the data to determine the thermodynamics of halogen bond formation. The ^{19}F chemical shift of

the metal fluoride resonance is very sensitive to adduct formation, moving ~ 35 ppm downfield in the limit for the 1:1 adduct. There is no evidence for a 1:2 adduct. The value of J_{PtF} increases from about 245 in the free molecule to about 360 Hz in the adduct of $\text{trans}[\text{Pt}(\text{F})\{2\text{-C}_5\text{NF}_2\text{H}(\text{CF}_3)\}_2(\text{P}^i\text{Pr}_3)_2]$ **4b**. We have shown that a comparison of the thermodynamics of binding for these structurally similar complexes is acceptable due to the negligible influence of the pyridyl substituents on the thermodynamic data. The identity of the phosphine has a much more marked influence on the thermodynamics. The value of $-\Delta H^\circ$ increases markedly from Ni to Pd to Pt ($-\Delta H^\circ$ Ni 18.9, Pd 21.7, Pt 24.5 kJ mol^{-1}). The values of ΔS° range from -54 to $-73 \text{ J K}^{-1} \text{ mol}^{-1}$ for the corresponding complexes, but the correlation of ΔS° with $-\Delta H^\circ$ is less than perfect, rendering it hard to discern systematic trends. The trends in the equilibrium constants are significantly different from those in $-\Delta H^\circ$, making the value of temperature-dependent data clear. At 300 K, the equilibrium constants range from 2.4 to 5.2, while at 200 K they range from 72 to 385. Although the biggest equilibrium constant at 300 K is found for palladium complex **3**, the biggest equilibrium constant below 200 K belongs to platinum complex **4a**. The trends in halogen bonding down a transition metal group may be compared with trends in dihydrogen bonding. The best examples are probably those of $\text{M}(\text{P}(\text{CH}_2\text{CH}_2\text{PPh}_2)_3(\text{H})_2)$ (M = Fe, Ru, Os) interacting with alcohols which also demonstrate a trend of increasing $-\Delta H^\circ$ down the group.^{17d}

The DFT studies of halogen bonding provide estimates of the interaction enthalpy of halogen bonding of $-18.8 \text{ kJ mol}^{-1}$ and $-22.8 \text{ kJ mol}^{-1}$ for models of **5a** (Ni) and **4a** (Pt), respectively, using PMe_3 in place of PCy_3 . These compare with the experimental values of ΔH° of $-18.9(4)$ and $-24.5(11) \text{ kJ mol}^{-1}$ for **5a** (Ni) and **4a** (Pt). The calculated $\text{I}\cdots\text{F}(\text{M})$ distance is slightly shorter for M = Pt, in keeping with the stronger halogen bond. The calculations show a bond critical point between F and I, and a very marked region of negative potential around fluorine.

In summary, we have found that these group 10 metal fluorides are excellent halogen bond acceptors, giving enthalpies for these interactions that are even greater than the value obtained in previous studies for $\text{trans}[\text{Ni}(\text{F})(2\text{-C}_5\text{NF}_4)(\text{PEt}_3)_2]$. Moreover, these data provide quantitative data that may be compared with models and imply that halogen bonding is a force comparable in strength to hydrogen bonding.

EXPERIMENTAL SECTION

General Procedures. All operations were performed under an argon atmosphere, either on a high-vacuum line (10^{-4} mbar) using modified Schlenk techniques, on standard Schlenk lines (10^{-2} mbar) or in a glovebox. Solvents for general use (*n*-hexane, toluene) were of AR grade, dried by distillation over standard reagents, or with a solvent purification system, and stored under Ar in ampules fitted with Young's PTFE stopcocks.

Deuterated solvents were dried by stirring over potassium, and were distilled under high vacuum into small ampules with potassium mirrors. All NMR spectra were recorded on Bruker AMX500 spectrometers in the same type of tube. All ^1H NMR spectra were recorded at 500.2 MHz; chemical shifts are reported in ppm (δ) relative to tetramethylsilane and are referenced using the chemical shifts of residual protio solvent resonances (benzene, δ 7.16). The $^{31}\text{P}\{^1\text{H}\}$ NMR spectra were recorded at 202.5 MHz and are referenced to external H_3PO_4 . ^{19}F NMR spectra were recorded at 470.5 MHz and referenced to external CFCl_3 at δ 0 or internal C_6F_6 at δ -162.9 . The temperature of the probe was calibrated according to

published procedures.³⁶ Mass spectra were recorded by the University of York analytical services on a Waters GCT instrument fitted with a Linden LIFDI probe and are quoted for ⁵⁸Ni. Infrared spectra were recorded as KBr disks (prepared in the glovebox) on a Unicam-Mattson Research Series FTIR spectrometer fitted with a KBr beam splitter. The sample chamber was purged with dry, CO₂-free air. Samples for elemental analysis were prepared in a glovebox, sealed under vacuum, and measured by Elemental Microanalysis Ltd., Okehampton. Chemicals were obtained from the following sources: bis(1,5-cyclooctadiene)-nickel(0), iodopentafluorobenzene, and potassium tetrachloroplatinate from Aldrich (or recovered from platinum residues by a standard procedure); allylpalladium chloride dimer, PiPr₃, and PCy₃ from Strem, pentafluoropyridine and 2,3,5-trifluoro-4-trifluoromethyl-pyridine from Fluorochem. *trans*-[Pd(F)(4-C₅NF₄)(PCy₃)₂] (**3**),^{20a} *trans*-[Pt(F){2-C₅NF₂H(CF₃)}(PCy₃)₂] (**4a**),^{20b} and *trans*-[Pt(F){2-C₅NF₂H(CF₃)}(PiPr₃)₂] (**4b**)^{20b} were synthesized according to known literature procedures.

trans-[Ni(F)(2-C₅NF₄)(PCy₃)₂] (**2**). Ni(COD)₂ (0.500 g, 1.82 mmol) and PCy₃ (1.274 g, 4.54 mmol) were suspended in 15 mL of *n*-hexane. The orange-red mixture was stirred for 10 min at room temperature, and pentafluoropyridine (0.240 mL, 2.19 mmol) was added at this temperature. The color of the reaction mixture changed to orange. After 2 h of stirring at room temperature, the suspension was filtered to give an orange solution. Storage at -25 °C overnight yielded yellow crystals, which were isolated, washed with cold *n*-hexane, and dried under vacuum; yield: 0.94 g (1.19 mmol, 66%). Anal. Calcd for C₄₁H₆₆F₅NNiP₂ (rmm 788.6): C, 62.44; H, 8.44; N, 1.78. Found: C, 62.92; H, 7.80; N, 1.86. IR (KBr disk, cm⁻¹): 1620 (m), 1595 (m), 1581 (s), 1481 (s), 1449 (s), 1420 (s), 1402 (s), 1381 (s), 1342 (m), 1266 (m), 1199 (m), 1174 (m), 1125 (m), 1085 (s), 1048 (w), 1003 (m), 994 (vs), 915 (m), 848 (s), 806 (vs), 736 (s), 711 (w), 676 (w), 605 (w), 530 (s), 513 (s), 491 (m), 450 (w), 407 (w). NMR: ¹H (300 K, benzene-*d*₆): δ 0.8–2.2 (m, C₆H₁₁). ¹⁹F (300 K, benzene-*d*₆): δ -378.0 (t, *J*_{FF} = 37 Hz, 1F, NiF), -175.1 (m, 1F, F⁵), -152.7 (m, 1F, F⁴), -126.6 (t, *J*_{FF} = 28 Hz, 1F, F³), -85.8 (m, 1F, F⁶). ³¹P (300 K, benzene-*d*₆): δ 19.3 (d, *J*_{PF} = 37 Hz). MS, *m/z* (LIFDI⁺): 787.6 (M⁺) 100%, 769.6 (MH - F)⁺ 16%.

trans-[Ni(F){2-C₅NF₂H(CF₃)}(PCy₃)₂] (**5a**). Ni(COD)₂ (0.248 g, 0.90 mmol) and PCy₃ (0.505 g, 1.80 mmol) were suspended in 10 mL of *n*-hexane. The orange-red mixture was stirred for 10 min at room temperature, and 2,3,5-trifluoro-4-trifluoromethyl-pyridine (0.200 g, 0.99 mmol) was added at this temperature. The color of the reaction mixture changed to red, and after one hour a yellow precipitate formed. The solid was separated by filtration, washed with *n*-hexane, and dried in vacuum. Crystals suitable for X-ray analysis were obtained from saturated toluene solutions at room temperature; yield: 0.589 g (0.72 mmol, 79%). Anal. Calcd for C₄₂H₆₇F₆NNiP₂ (rmm 820.62): C, 61.47; H, 8.23; N, 1.71. Found: C, 61.01; H, 8.24; N, 1.60. IR (KBr disk, cm⁻¹): 1595 (m), 1542 (m), 1466 (m), 1446 (s), 1352 (s), 1340 (s), 1296 (s), 1266 (m), 1227 (w), 1194 (m), 1171 (s), 1143 (s), 1108 (m), 1079 (s), 1048 (w), 1025 (s), 1003 (m), 914 (w), 887 (w), 848 (m), 804 (w), 766 (w), 736 (s), 708 (s), 664 (s), 649 (m), 575 (s), 563 (m), 511 (s), 489 (m), 450 (w). NMR: ¹H (300 K, benzene-*d*₆): δ 0.8–2.3 (m, 66H, C₆H₁₁), 8.50 (s, 1H, H-pyridyl). ¹⁹F (300 K, benzene-*d*₆): δ -375.1 (t, *J*_{FF} = 39 Hz, 1F, NiF), -146.3 (q, *J*_{FF} = 21 Hz, 1F, *p*-F), -101.0 (q, 1F, *J*_{FF} = 20 Hz, *o*-F), -56.8 (t, 1F, *J*_{FF} = 21 Hz, CF₃). ³¹P (300 K, benzene-*d*₆): δ 19.0 (d, *J*_{PF} = 39 Hz). MS, *m/z* (LIFDI⁺): 819.4 (M⁺) 100%.

trans-[Ni(F){2-C₅NF₂H(CF₃)}(PCyp₃)₂] (**5c**). This complex was prepared in a fashion identical to that for the synthesis of (**5a**). Yield 0.97 g (1.22 mmol, 72%). Anal. Calcd for C₃₆H₅₅F₆NNiP₂ (rmm 736.46): C, 58.71; H, 7.53; N, 1.90. Found C, 58.52; H, 7.72; N, 1.86. IR (KBr disk, cm⁻¹): 2952 (vs), 2868 (s), 1996 (w), 1540 (w), 1449 (m sharp), 1355 (s sharp), 1297 (vs sharp), 1166 (m), 1140 (vs), 1080 (w), 1025 (m), 921 (w), 804 (w), 708 (w) 665 (w), 548 (w), 500 (m). NMR ¹H (300 K, benzene-*d*₆): δ 1.5–2.3 (m, 54H, C₅H₉), 8.52 (s, 1H, H-Pyridyl). ¹⁹F (300 K, benzene-*d*₆): δ -377.62 (t, 1F, *J*_{PF} = 40.8 Hz, Pt-F),

-145.85 (q, 1F, *J*_{FF} = 22.2 Hz, *p*-F), -102 (q, 1F, *J*_{FF} = 22.5 Hz *o*-F), -57.2 (t, *J*_{FF} = 20 Hz, 3F, CF₃), ³¹P (300 K, benzene-*d*₆): δ 17.7 (*J*_{PF} = 41 Hz). MS *m/z* (LIFDI⁺): 735.3 (M⁺) 100%.

X-ray Crystallography. Diffraction data were collected on a Bruker SMART APEX I diffractometer with Mo K α radiation (λ = 0.71073 Å). Diffractometer control, data collection, and initial unit cell determination were performed using "SMART" (v5.625, Bruker AXS). Frame integration and unit cell refinement were carried out with "SAINT+" (v6.22, Bruker AXS). Absorption corrections were applied empirically (SADABS, v.2.10) based upon symmetry-equivalent reflections combined with measurements at different azimuthal angles.³⁷ The structures were solved by direct methods using SHELXS-97 and refined by full-matrix least-squares methods using SHELXL-97.³⁸ Hydrogen atoms were placed at calculated positions and were included in the refinement using a riding model. For complex **2**, the crystals exhibited disorder of both the perfluoropyridyl ligand and the toluene of crystallization. Each was modeled over two sites with relative occupancy 63.9:36.1(6). For the toluene, the aromatic C–C bond lengths restrained to be equal. For complex **5a**, the structure was modeled with the CF₃ group disordered over two positions in a 81.7:18.3(4) ratio. The C–F bonds of this group were restrained to 1.34 Å and the distances between F atoms of the same residue restrained to be equal. The atomic displacement factor of F(5a) was restrained to be approximately isotropic. Large ADP max/min ratios are explained as a consequence of rotation about the CF₃ axis. For complex **5c**, the CF₃ group was disordered and modeled over two positions the relative occupancy of which refined to 63.7:36.3(4). Three of the cyclopentyl groups exhibited disorder and for each group one carbon atom was modeled in two positions (C(19/19a), C(25/25a), and C(35/35a)) the relative occupancy of which refined to 0.545:0.455(7), 0.736:0.264(8), and 0.558:0.442(8), respectively. See Table 3 for data for **2**, **5a**, and **5c**.

NMR Titrations and Analysis of Data. The equilibrium constants were determined through NMR titration at a series of temperatures, by following the chemical shift of the fluoride ligand coordinated to the transition metal. The volumes of the solutions were assumed to be the sum of the volumes of the components, thereby enabling the densities of the solutions to be calculated. Test solutions of iodopentafluorobenzene in protio-toluene, in concentrations similar to those used in the titrations, showed no significant deviation from this assumption. The activities of the species were assumed equal to their molar concentration. The calculations for the equilibrium constants were carried out with Microsoft Excel, using a macro programmed by Prof. Christopher A. Hunter of the University of Sheffield. There are two parameters to be fitted: the equilibrium constant *K* and the downfield shift from the signal of free metal fluoride for the coordinated fluoride in the adduct, $\Delta\delta^{\text{fit}}$. The two parameters can be fitted for the whole range of temperatures without any restraints. ΔH° and ΔS° were calculated from the Van't Hoff plots of the equilibrium constants.

General Procedure for the Preparation of the NMR Samples. The solutions for titration were prepared as follows. A solution of known concentration of the metal fluoride was prepared by dissolving the complex in toluene, and a solution of C₆F₅I (the titrant solution, also of known concentration, see Table S1 in SI) by dissolving C₆F₅I in toluene. Approximately equal amounts of the solution of the complex were transferred into each of ten labeled NMR tubes in the glovebox; the mass of the solution contained in each tube was recorded. In one sample, no C₆F₅I solution was added, providing a reference; in the other tubes, variable amounts of the solution of C₆F₅I were added by volume, in quantities ranging from 5 μ L up to 160 μ L. The ¹⁹F NMR spectra of all samples were recorded at various temperatures. The samples were kept in a bath close to the temperature of the probe and left to equilibrate inside the probe for two minutes before the spectrum was recorded. The ¹⁹F NMR spectra were collected unlocked. However, for each temperature the spectrometer was shimmed with a solution of the corresponding

Table 3. Crystallographic Data for Complexes **2**, **5a**, and **5c**

	2 ·toluene	5a	5c
cryst syst	orthorhombic	monoclinic	monoclinic
space group	<i>Pmn</i> 2 ₁	<i>P</i> 2 ₁ / <i>c</i>	<i>P</i> 2 ₁ / <i>n</i>
formula	C ₄₁ H ₆₆ F ₅ NNiP ₂ ·C ₇ H ₈	C ₄₂ H ₆₇ F ₆ NNiP ₂	C ₃₆ H ₅₅ F ₆ NNiP ₂
<i>a</i> [Å]	13.9158(12)	13.6755(13)	14.5066(3)
<i>b</i> [Å]	16.9189(14)	18.4389(17)	12.3458(2)
<i>c</i> [Å]	9.7820(8)	17.6985(16)	19.7390(3)
β [deg]	90.00	111.439(2)	91.3446(17)
<i>V</i> [Å ³]	2303.1(3)	4154.1(7)	3534.18(12)
<i>Z</i>	2	4	4
density [g cm ⁻³]	1.270	1.312	1.384
μ (Mo K α) [mm ⁻¹]	0.544	0.601	0.698
<i>T</i> [K]	110(2)	110(2)	110(2)
no. of rflns (measd)	25854	42705	19381
no. of rflns (indep)	6904	10329	10333
no. of rflns (obsd and used in refinement, <i>n</i>)	5924	8147	8174
no. of params, <i>p</i>	332	497	455
GOF on <i>F</i> ² (all data)	1.016	1.036	1.038
<i>R</i> ₁ (<i>F</i>) (<i>I</i> > 2 σ (<i>I</i>))	0.0348	0.0434	0.0398
<i>wR</i> ₂ (<i>F</i> ²) (all data)	0.0816	0.1139	0.0831
CCDC number	831711	831710	831709

metal fluoride in toluene-*d*₈ and maintained with the same settings throughout.

For the Job plots, a stock solution of C₆F₅I in toluene of concentration 0.01 mol dm⁻³ was prepared in the glovebox. A stock solution of the metal complex was prepared with the same concentration. NMR tubes were made up with measured aliquots of each solution such that the total volume in the NMR tube was 0.400 mL.

Computational Methods. All calculations were performed using density functional theory as implemented in the Gaussian03 package.³⁹ The BHandHLYP functional was used in conjunction with the SDD effective core potential and associated basis set on P, Ni, and Pt and a 6-31G* basis on all main group atoms. This functional has been shown to provide accurate energetics for noncovalently bonded systems.⁴⁰ Diffuse functions were also added to all fluorine atoms (6-31+G*). All phosphine ligands were modeled as PMe₃. Equilibrium structures were fully optimized, including counterpoise corrections, starting from a geometry where the C–I and F–M groups were colinear. An ultrafine grid was used together with tight optimization criteria. Frequency calculations confirmed all reported stationary points to be minima, although in the case of the adducts, three low-lying modes were present that related to the bending of the C₆F₅I unit relative to the metal complex. Interaction enthalpies were corrected for basis set superposition error (BSSE) using the counterpoise correction of Boys, and also for the effect of zero-point energies.

■ ASSOCIATED CONTENT

Supporting Information. Crystallographic data for **2**, **5a**, and **5c**; titration data and Van't Hoff plots for **3**, **4a**, **4b** and **5b**; Job plots for **2** and **4a**; temperature dependence of derived equilibrium constants for C₆F₅I adducts; ³¹P{¹H} and ¹⁹F NMR spectra of **5c**; ¹⁹F NMR spectra of **4b** in presence and absence of C₆F₅I; author list for Gaussian 03 (ref 39), packing diagram for **5a** showing short Ni–F···H–C hydrogen bonds. Cartesian coordinates and total energies for all computed structures. This material is available free of charge via the Internet at <http://pubs.acs.org>.

■ AUTHOR INFORMATION

Corresponding Author

robin.perutz@york.ac.uk

Present Addresses

¹Leibniz-Institut für Katalyse e.V. an der Universität Rostock, Albert-Einstein-Strasse 29a, 18059 Rostock, Germany.

■ ACKNOWLEDGMENT

This work was supported by the Deutsche Forschungsgemeinschaft (research fellowship for T.B., Grant No. BE 4370/1-1) and the EPSRC. We thank Dr. Marius V. Câmpian (University of York), Stefano Libri (University of Sheffield), and Robert J. Thatcher (University of York) for discussions and suggestions, and Jason Loader (University of Sheffield) for preparation of electrostatic potential diagrams. Prof. Christopher A. Hunter (University of Sheffield) provided the macro used in calculation of the equilibrium constants and help with the application of the program.

■ REFERENCES

- (1) (a) Brammer, L.; Bruton, E. A.; Sherwood, P. *Cryst. Growth Des.* **2001**, *1*, 277. (b) Steiner, T. *Angew. Chem., Int. Ed.* **2002**, *41*, 48. (c) Desiraju, G. R.; Steiner, T. *The Weak Hydrogen Bond*; Oxford University Press: Oxford, 1999.
- (2) (a) Metrangolo, P.; Neukirch, H.; Pilati, T.; Resnati, G. *Acc. Chem. Res.* **2005**, *38*, 386. (b) Metrangolo, P.; Resnati, G., Eds. *Halogen Bonding: Fundamentals and Applications, Structure & Bonding*; Springer: Berlin, 2007. (c) Metrangolo, P.; Meyer, F.; Pilati, T.; Resnati, G.; Terraneo, G. *Angew. Chem., Int. Ed.* **2008**, *47*, 6114. (d) Brammer, L.; Minguez Espallargas, G.; Libri, S. *CrystEngComm* **2008**, *10*, 1712. (e) Metrangolo, P.; Carcenac, Y.; Lahtinen, M.; Pilati, T.; Rissanen, K.; Vij, A.; Resnati, G. *Science* **2009**, *323*, 1461. (f) Fourmigué, M. *Curr. Opin. Solid State Mater. Sci.* **2009**, *13*, 36. (g) Ritter, S. K. *Chem. Eng. News* **2009**, *87*, 39.

- (3) (a) Brammer, L.; Swearingen, J. K.; Bruton, E. A.; Sherwood, P. *Proc. Nat. Acad. Sci., U.S.A.* **2002**, *99*, 4956. (b) Mareque Rivas, J. C.; Brammer, L. *Inorg. Chem.* **1998**, *37*, 4746. (c) Lewis, G. R.; Orpen, A. G. *Chem. Commun.* **1998**, 1873. (d) Banerjee, R.; Desiraju, G. R.; Mondal, R.; Howard, J. A. K. *Chem.—Eur. J.* **2004**, *10*, 3373. (e) Walsh, R. B.; Padgett, C. W.; Metrangolo, P.; Resnati, G.; Hanks, T. W.; Pennington, W. T. *Cryst. Growth Des.* **2001**, *1*, 165. (f) Bosch, E.; Barnes, C. L. *Cryst. Growth Des.* **2002**, *2*, 299. (g) Brammer, L.; Mínguez Espallargas, G.; Adams, H. *CrystEngComm* **2003**, *5*, 343. (h) Zordan, F.; Brammer, L.; Sherwood, P. *J. Am. Chem. Soc.* **2005**, *127*, 5979. (i) Mínguez Espallargas, G.; Brammer, L.; Sherwood, P. *Angew. Chem., Int. Ed.* **2006**, *45*, 435. (j) Rosokha, S. V.; Neretin, I. S.; Rosokha, T. Y.; Hecht, J.; Kochi, J. K. *Heteratom. Chem.* **2006**, *17*, 449. (k) Derossi, S.; Brammer, L.; Hunter, C. A.; Ward, M. D. *Inorg. Chem.* **2009**, *48*, 1666.
- (4) Laguna, A.; Lasanta, T.; López-de-Luzuriaga, J. M.; Monge, M.; Naumov, P.; Olmos, M. E. *J. Am. Chem. Soc.* **2010**, *134*, 456.
- (5) (a) Corradi, E.; Meille, S. V.; Messina, M. T.; Metrangolo, P.; Resnati, G. *Angew. Chem., Int. Ed.* **2000**, *39*, 1782. (b) Sun, A. W.; Lauher, J. W.; Goroff, N. S. *Science* **2006**, *312*, 5776. (c) Shirman, T.; Arad, T.; van der Boom, M. E. *Angew. Chem., Int. Ed.* **2010**, *49*, 926. (d) Serpell, C. J.; Kilah, N. L.; Costa, P. J.; Felix, V.; Beer, P. D. *Angew. Chem., Int. Ed.* **2010**, *49*, 5322. (e) Kilah, N. L.; Wise, M. D.; Serpell, C. J.; Thompson, A. L.; White, N. G.; Christensen, K. E.; Beer, P. D. *J. Am. Chem. Soc.* **2010**, *132*, 11893.
- (6) (a) Nguyen, H. L.; Horton, P. N.; Hursthouse, M. B.; Legon, A. C.; Bruce, D. W. *J. Am. Chem. Soc.* **2004**, *126*, 16. (b) Präsang, C.; Whitwood, A. C.; Bruce, D. W. *Chem. Commun.* **2008**, 2137.
- (7) (a) Fourmigué, M.; Batail, P. *Chem. Rev.* **2004**, *104*, 5379. (b) Imakubo, T.; Sawa, H.; Kato, R. *J. Chem. Soc., Chem. Commun.* **1995**, 1667. (c) Yamamoto, H. M.; Kosaka, Y.; Maeda, R.; Yamaura, J.; Nakao, A.; Nakamura, T.; Kato, R. *ACS Nano* **2008**, *2*, 143.
- (8) (a) Auffinger, P.; Hays, F. A.; Westhof, E.; Ho, P. S. *Proc. Nat. Acad. Sci. U.S.A.* **2004**, *101*, 16789. (b) Howard, E.; Sanishvili, R.; Cachau, R. E.; Mitschler, B.; Bart, P.; Lamour, V.; Van Zandt, M.; Sibley, E.; Bon, C.; Moras, D.; Schneider, T. R.; Joachimiak, A.; Podjarny, A. *Proteins Struct., Funct., Genet.* **2004**, *55*, 792. (c) Parisini, E.; Metrangolo, P.; Pilati, T.; Resnati, G.; Terraneo, G. *Chem. Soc. Rev.* **2011**, *40*, 2267.
- (9) (a) Legon, A. C. *Angew. Chem., Int. Ed.* **1999**, *38*, 2686. (b) Legon, A. C. *Phys. Chem. Chem. Phys.* **2010**, *12*, 7736.
- (10) (a) Clark, T.; Hennemann, M.; Murray, J. S.; Politzer, P. *J. Mol. Model* **2007**, *13*, 291. (b) Politzer, P.; Murray, J. S.; Clark, T. *Phys. Chem. Chem. Phys.* **2010**, *12*, 7748.
- (11) (a) Mínguez Espallargas, G.; Zordan, F.; Arroyo Marin, L.; Adams, H.; Shankland, K.; van de Streek, J.; Brammer, L. *Chem.—Eur. J.* **2009**, *15*, 7554. (b) Reddy, L. S.; Chandran, S. K.; George, S.; Babu, N. J.; Nangia, A. *Cryst. Growth Des.* **2007**, *7*, 2675. (c) Aakeröy, C. B.; Fasulo, M.; Schulteiss, N.; Desper, J.; Moore, C. *J. Am. Chem. Soc.* **2007**, *129*, 13772.
- (12) (a) Laurence, C.; Queignec-Cabanatos, M.; Dziembowska, T.; Queignec, R.; Wojtkowiak, B. *J. Am. Chem. Soc.* **1981**, *103*, 2567. (b) Laurence, C.; Queignec-Cabanatos, M.; Wojtkowiak, B. *J. Chem. Soc., Perkin Trans. 2* **1982**, 1605. (c) Laurence, C.; Quegnec-Cabanatos, M.; Woirowiak, B. *Can. J. Chem.* **1983**, *61*, 135.
- (13) (a) Cabot, R.; Hunter, C. A. *Chem. Commun.* **2009**, 2005. (b) Sarwar, M. G.; Dragisic, B.; Salsberg, L. J.; Gouliaras, C.; Taylor, M. S. *J. Am. Chem. Soc.* **2010**, *134*, 1646. (c) Dimitrijević, E.; Kvak, O.; Taylor, M. S. *Chem. Commun.* **2010**, *46*, 9025. (d) Hauchecorne, D.; van der Veken, B. J.; Herrebout, W. A.; Hansen, P. E. *Chem. Phys.* **2011**, *38*, 5.
- (14) Libri, S.; Jasim, N. A.; Perutz, R. N.; Brammer, L. *J. Am. Chem. Soc.* **2008**, *130*, 7842.
- (15) (a) Murphy, E. F.; Murugavel, R.; Roesky, H. W. *Chem. Rev.* **1997**, *97*, 3425. (b) Braun, T.; Perutz, R. N. *Chem. Commun.* **2002**, 2749. (c) Braun, T.; Perutz, R. N. *Transition-Metal Mediated C—F Bond Activation*. In *Comprehensive Organometallic Chemistry III*; Crabtree, R. H.; Mingos, D. M. P., Eds.; Elsevier: Amsterdam, 2006; Vol. 1, Chapter 26. (d) Clot, E.; Eisenstein, O.; Jasim, N.; Macgregor, S. A.; McGrady, J. E.; Perutz, R. N. *Acc. Chem. Res.* **2011**, *44*, 333.
- (16) (a) Ball, N. D.; Sanford, M. S. *J. Am. Chem. Soc.* **2009**, *128*, 7134. (b) Watson, D. A.; Su, M.; Teverovskiy, G.; Zhang, Y.; García-Fortanet, J.; Kinzel, T.; Buchwald, S. L. *Science* **2009**, *325*, 1661. (c) Engle, K. M.; Mei, T.-S.; Wang, X.; Yu, J.-Q. *Angew. Chem., Int. Ed.* **2011**, *50*, 1478.
- (17) (a) Richmond, T. G. *Coord. Chem. Rev.* **1990**, *105*, 221. (b) Yandulov, D. V.; Caulton, K. G.; Belkova, N. V.; Shubina, E. S.; Epstein, L. M.; Khoroshum, D. V.; Musaev, D. G.; Morokuma, K. *J. Am. Chem. Soc.* **1998**, *120*, 12553. (c) Lee, D.-H.; Kwon, H. J.; Patel, B. P.; Liable-Sands, L. M.; Rheingold, A. L.; Crabtree, R. H. *Organometallics* **1999**, *18*, 1615. (d) Gutsul, E. I.; Belkova, N. V.; Sverdlov, M. S.; Epstein, L. M.; Shubina, E. S.; Bakhmutov, V. I.; Gribova, T. N.; Minyaev, R. M.; Bianchini, C.; Peruzzini, M.; Zanobini, F. *Chem.—Eur. J.* **2003**, *9*, 2219. (e) Belkova, N. V.; Epstein, L. M.; Shubina, E. S. *Acc. Chem. Res.* **2005**, *38*, 624. (f) Brammer, L. *Dalton Trans.* **2003**, 3145.
- (18) *Examples of group 4 metal fluorides of the type Cp₂MF₂ and Cp^{*}₂MF₂*: (a) Druce, P. M.; Kingston, B. M.; Lappert, M. F.; Spalding, T. R.; Srivastava, R. C. *J. Chem. Soc. (A)* **1969**, 2106. (b) Herzog, A.; Liu, F.-Q.; Roesky, H. W.; Demsar, A.; Keller, K.; Noltemeyer, M.; Pauer, F. *Organometallics* **1994**, *13*, 1251. (c) Murphy, E. F.; Yu, P.; Dietrich, S.; Roesky, H. W.; Parisini, E.; Noltemeyer, M. *J. Chem. Soc., Dalton Trans.* **1996**, 1983.
- (19) Cronin, L.; Higgitt, C. L.; Karch, R.; Perutz, R. N. *Organometallics* **1997**, *16*, 4920.
- (20) (a) Jasim, N. A.; Perutz, R. N.; Whitwood, A. C.; Braun, T.; Izundu, J.; Neumann, B.; Rothfeld, S.; Stammler, H.-G. *Organometallics* **2004**, *23*, 6140. (b) Nova, A.; Erhardt, S.; Jasim, N. A.; Perutz, R. N.; Macgregor, S. A.; McGrady, J. E.; Whitwood, A. C. *J. Am. Chem. Soc.* **2008**, *130*, 15499.
- (21) Nova, A.; Reinhold, M.; Perutz, R. N.; Macgregor, S. A.; McGrady, J. E. *Organometallics* **2010**, *29*, 1824.
- (22) Dransfield, T. A.; Nazir, P.; Perutz, R. N.; Whitwood, A. C. *J. Fluorine Chem.* **2010**, *131*, 1213.
- (23) (a) A survey of crystal structures (CSD Conquest 1.12; Nov 2009 + 1 update)^{23b} of square-planar bis(phosphines)nickel and bis(phosphines)platinum complexes containing a monodentate O-bonded ligand show the same trend for M—O distances, viz. mean Ni—O 1.899 Å (40 observations) and mean Pt—O 2.107 Å (114 observations); $\Delta d = 0.208$ Å. (b) Allen, F. H. *Acta Crystallogr.* **2002**, *B58*, 380.
- (24) (a) Su, M.-D.; Chu, S.-Y. *J. Am. Chem. Soc.* **1997**, *119*, 10178. (b) Bosque, R.; Clot, E.; Fantacci, S.; Maseras, F.; Eisenstein, O.; Perutz, R. N.; Renkema, K. B.; Caulton, K. G. *J. Am. Chem. Soc.* **1998**, *120*, 12634. (c) Su, M.-D.; Chu, S.-Y. *J. Am. Chem. Soc.* **1999**, *121*, 1045. (d) Gérard, H.; Davidson, E. R.; Eisenstein, O. *Mol. Phys.* **2002**, *100*, 533. (e) Gérard, H.; Eisenstein, O. *Dalton Trans.* **2003**, 839. (f) Reinhold, M.; McGrady, J. E.; Perutz, R. N. *J. Am. Chem. Soc.* **2004**, *126*, 5268.
- (25) Valerio, G.; Raos, G.; Meille, S. V.; Metrangolo, P.; Resnati, G. *J. Phys. Chem. A* **2000**, *104*, 1617.
- (26) For examples of similar methodology for Job plots, see (a) McCall, A. S.; Wang, H.; Desper, J. M.; Kraft, S. *J. Am. Chem. Soc.* **2011**, *1330*, 1832. (b) Yoo, H.; Mirkin, C. A.; DiPasquale, A. G.; Rheingold, A. L.; Stern, C. L. *Inorg. Chem.* **2008**, *47*, 9727.
- (27) (a) Williams, J. H. *Acc. Chem. Res.* **1993**, *26*, 593. (b) Reichenbacher, K.; Süß, H. I.; Hulliger, J. *Chem. Soc. Rev.* **2005**, *34*, 22. (c) Coates, G. W.; Dunn, A. R.; Henling, L. M.; Ziller, J. W.; Lobkovsky, E. B.; Grubbs, R. H. *J. Am. Chem. Soc.* **1998**, *120*, 3641. (d) Vanspeybrouck, W.; Herrebout, W. A.; van der Veken, B. J.; Lundell, J.; Perutz, R. N. *J. Phys. Chem. B* **2003**, *107*, 13855.
- (28) (a) Khandogin, J.; Ziegler, T. *Spectrochim. Acta, Part A* **1999**, *55*, 607. (b) Feindel, K. W.; Wasylishen, R. E. *Magn. Reson. Chem.* **2004**, *42*, S158.
- (29) We are aware that the Fermi Contact term and the paramagnetic spin—orbital term derive principally from covalent bonding rather than from electrostatic perturbation. We have considered several possible scenarios: for instance, the paramagnetic spin—orbital term should be strongly affected by the energy separation between d_{xy} and $d_{x^2-y^2}$ orbitals. This energy gap may be influenced by an electric field gradient within an electrostatic model, or by a small covalent component.
- (30) Bondi, A. *J. Phys. Chem.* **1964**, *68*, 441.

(31) $R_{IF} = d(I \cdots F) / r_I + r_F$, where r_I and r_F are, respectively, the van der Waals radii of I and F, following the definition in Lommerse, J. P. M.; Stone, A. J.; Taylor, R.; Allen, F. H. *J. Am. Chem. Soc.* **1996**, *118*, 3108.

(32) (a) Pt is more electronegative than Ni.^{32b} (b) Huheey, J. E.; Keiter, E. A.; Keiter, R. L. *Inorganic Chemistry, Principles of structure and reactivity*, 4th Ed; Harper Collins: New York, 1993.

(33) (a) Bader, R. F. W. *Atoms in Molecules: A Quantum Theory*, Oxford University Press: Oxford, 1990. (b) Popelier, P. *Atoms in Molecules, An Introduction*; Pearson Education, Harlow: New York, 2000. (c) Bader, R. F. W. *Chem. Rev.* **1991**, *91*, 893.

(34) Martinez Amezaga, N. J.; Pamies, S. C.; Peruchena, N. M.; Sosa, G. L. *J. Phys. Chem. A* **2010**, *114*, 552.

(35) Lu, Y.-X.; Zou, J.-W.; Wang, Y. H.; Jiang, Y.-J.; Yu, Q.-S. *J. Phys. Chem. A* **2007**, *111*, 10781.

(36) Ammann, C.; Meier, P.; Merbach, A. E. *J. Magn. Reson.* **1982**, *46*, 319.

(37) (a) Sheldrick, G. M. *SADABS: Empirical absorption correction program*; University of Göttingen: Göttingen, 1995, based upon the method of Blessing.^{37b} (b) Blessing, R. H. *Acta Crystallogr.* **1995**, *A51*, 33.

(38) Sheldrick, G. M. *Acta Crystallogr.* **2008**, *A64*, 112.

(39) Frisch, M. J. et al. . *Gaussian 03*, Revision C.02, Gaussian Inc: Wallingford CT, 2004.

(40) (a) Csontos, J.; Palermo, N. Y.; Murphy, R. F.; Lovas, S. *J. Comput. Chem.* **2008**, *29*, 1344. (b) Ruiz, E.; Salahub, D. R.; Vela, A. *J. Phys. Chem.* **1996**, *100*, 12265. (c) Piacenza, M.; Grimme, S. *J. Comput. Chem.* **2004**, *25*, 83. (d) Romero, C.; Fomina, L.; Fomine, S. *Int. J. Quantum Chem.* **2005**, *102*, 200. (e) Waller, M. P.; Robertazzi, A.; Platts, J. A.; Hibbs, D. E.; Williams, P. A. *J. Comput. Chem.* **2006**, *27*, 491.